IOP Conf. Series: Journal of Physics: Conf. Series **800** (2017) 012016 doi:10.1088/1742-6596/800/1/012016

Results on kaon physics from OKA setup at U-70 .

V Obraztsov, on behalf of the "OKA" collaboration

Institute for High Energy Physics, Protvino, Moscow Region, RU

E-mail: Vladimir.Obraztsov@ihep.ru

Abstract. Some recent results from OKA setup are presented. First, the decay $K^+ \to \pi^0 e^+ \nu(K_{e3})$ is studied. About 3.15M events are selected for the analysis. The linear and quadratic slopes for the decay formfactor $f_+(t)$ are measured: $\lambda'_+ = (26.1 \pm 0.45 \pm 0.38) \times 10^{-3}$, $\lambda''_+ = (1.94 \pm 0.23 \pm 0.12) \times 10^{-3}$. For the exotic scalar and tensor interactions we get: $F_S/f_+(0) = (-0.44 \pm 0.7 \pm 0.24) \times 10^{-2}$; $F_T/f_+(0) = (0.16 \pm 2 \pm 1.3) \times 10^{-2}$. Several alternative parametrizations are tried: the Pole fit parameter is found to be $M_V = 890 \pm 3.7$ MeV ; the parameter of the Dispersive parametrization is measured to be $\Lambda_+ = (24.72 \pm 0.23) \times 10^{-3}$. Second, the results of a search for heavy neutrino in the $K_{\mu 2}$ decay are shown. The upper limits on the mixing parameter of the heavy neutrino with the muon neutrino $|U_{\mu H}|^2$ are obtained. Typically, $|U_{\mu H}|^2 \leq 10^{-6}$ for the region $225 \leq m_H \leq 375$ MeV. Third, a new study of the radiative $K_{\mu 3}$ decay are presented. The number of signal events is ~ 580 which is 4 times larger than in previous measurements. $R = Br(K^+_{\mu 3\gamma}, 30 < E_\gamma < 60 MeV)/Br(K_{\mu 3}) = (4.85 \pm 0.2(stat) \pm 0.5(syst)) \times 10^{-4}$ which should be compared with 4.7×10^{-4} from the theory. An estimate of the T-odd asymmetry gives $A_\xi = (-0.19 \pm 0.05 \pm 0.09)$. A space asymmetry over $cos(\theta^*_{\mu\gamma})$, where $\theta^*_{\mu\gamma}$ is the angle between photon and muon momenta in the kaon rest frame is measured to be $A(cos\theta^*) = 0.6 \pm 0.05 \pm 0.1$.

1. Introduction

The kaon decays provide unique information about the dynamics of the strong interactions. It has been a testing ground for such theories as current algebra, PCAC, Chiral Perturbation Theory (ChPT) etc. Another direction is a search for new physics: new light particles and new interactions. In this talk, we present a high-statistics study of K_{e3}; $K_{\mu 2}$ and $K_{\mu 3}\gamma$ decays from OKA detector at U-70 Proton Synchrotron.

2. OKA beam and detector

OKA is the abbreviation for 'Experiments with Kaons '. OKA beam is a RF-separated secondary beam of U-70 Proton Synchrotron of IHEP, Protvino. The beam is described elsewhere [1]. RF-separation with Panofsky scheme is realised. It uses two superconductive Karsruhe-CERN SC RF deflectors [2], donated by CERN. Sophisticated cryogenic system, built at IHEP [3] provides superfluid He for cavities cooling. The resulting beam has up to $\sim 20\%$ of kaons with an intensity of $\sim 10^6$ kaons per 3 sec U-70 spill. The OKA setup is a magnetic spectrometer, presented on Fig. 1. It includes:

(i) Beam spectrometer on the basis of 7 1mm pitch PC's ($BPC_{x,y}$) ~1500 channels in total, 4 2mm-thick scintillation counters and 2 threshold Cherenkov counters.

Figure 1. OKA setup

(ii) Decay volume(DV) with Veto system, 11m long, filled with He, veto system is composed of 670 Lead-Scintillator sandwiches 20×(5 mm Sc + 1.5 mm Pb) with WLS readout. The counters are grouped in 300 ADC channels.

(iii) Main magnetic spectrometer: 200×140 cm^2 aperture magnet wih $\int Bdl \sim 1$ Tm; 5K 2 mm pitch PC's; 1K 9 mm Straw's and 300 channels of 40 mm DT's.

(iv) Gamma detectors: GAMS-2000 (~ 2000 4×4 cm^2 lead glass blocks), large angle detector (EGS) (~ 1500 4×4 cm^2 lead glass blocks).

(v) Muon detector: GDA-100 Hadron Calorimeter (100 20×20 cm^2 iron-scintillator sandwiches with WLS plates readout); 4 1×1 m^2 Sc counters behind GDA-100.

3. Trigger and statistics

Very simple trigger, which is almost ″minimum bias ″ one, has been used during data-taking: $Tr = S_1 \cdot S_2 \cdot S_3 \cdot \overline{\check{C}}_1 \cdot \check{C}_2 \cdot \overline{S}_{bk} \cdot (\Sigma_{GAMS} > MIP)$. It is a combination of beam Sc counters, $\check{C}_{1,2}$ threshold Cerenkov counters ($\check{C}_1$ sees pions, $\check{C}_2$- pions and kaons), S_{bk} - a ″beam-killer ″ counter located in the beam-hole of the GAMS gamma-detector. $\Sigma_{GAMS} > MIP$ is a requirement for the analog sum of amplitudes in the GAMS-2000 to be higher than a MIP signal.
The ″OKA″ is taking data since 2010, the total available statistics corresponds to $\sim 15MK_{e3}$ decays. In the present study we use part of the statistics taken in 2011 and 2012.

4. K_{e3} decay study.

The data processing starts with the beam particle reconstruction in $BPC_1 \div BPC_4$, then the secondary tracks are looked for in $PC_1 \div PC_8$; $ST_1 \div ST_3$; $DT_1 \div DT_2$ and events with one good positive track are selected. The decay vertex is searched for, and a cut is introduced on the matching of incoming and decay track. The next step is to look for showers in GAMS-2000 and EGS calorimeters. The electron identification is done using the ratio of the energy of the shower to the momentum of the associated track. The E/p distribution is shown in Fig. 2. The particles with $0.8 < \mathrm{E/p} < 1.2$ are accepted as electrons. The events with one charged track identified as electron and two additional showers in ECAL are selected for further processing. The mass spectrum of $\gamma\gamma$ shows a clean π^0 peak at $M_{\pi 0} = 134.9$ MeV with a resolution of ~ 8.5 MeV. To fight the main background from $K_{\pi 2}$ decay, the angle between the momentum of the beam kaon $\vec{p_K}$ and that of the $e\pi$-system i.e. $\vec{p_e} + \vec{p_\pi}$ is considered, see Fig. 2. The background is clearly seen as a peak at zero angles. The cut is $\alpha > 2$ mrad. Further selection is done by the requirement that the event passes 2C $K \to e\nu\pi^0$ fit. The event selection results in ∼3.15M events. The surviving background is estimated from MC to be less than 1%.

4.1. Analysis

The analysis is based on the fit of the distribution of the events over the Dalitz plot. The variables $y = 2E_e^*/M_K$ and $z = 2E_\pi^*/M_K$, where E_e^*, E_π^* are the energies of the electron and π^0 in the kaon

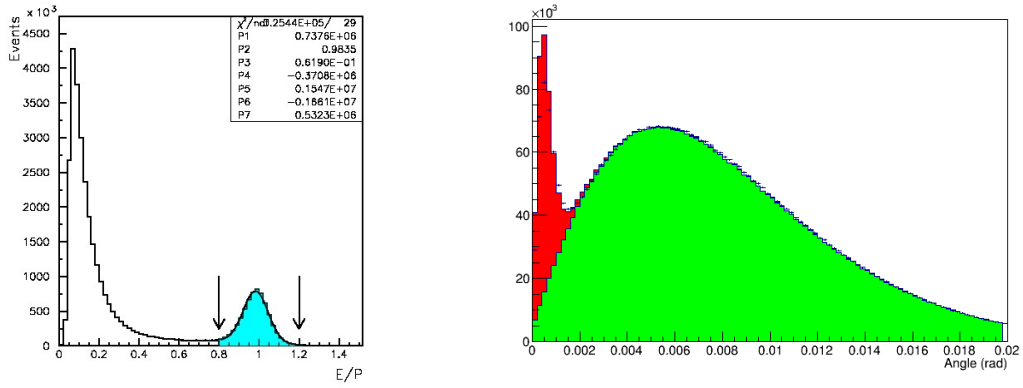

Figure 2. E/P plot - the ratio of the energy of the associated ECAL cluster to the momentum of the charged track (left); α - the angle between $\vec{p}_K$ and $\vec{p}_e + \vec{p}_\pi$ in the lab-system (right).

c.m.s are used. The background events, as MC shows, occupy the peripheral part of the plot. The most general Lorentz invariant form of the matrix element for the decay $K^+ \to l^+\nu\pi^0$ is [4]: $M = \frac{-G_F V_{us}}{2}\bar{u}(p_\nu)(1+\gamma^5)[((P_K+P_\pi)_\alpha f_+ + (P_K-P_\pi)_\alpha f_-)\gamma^\alpha - 2m_K f_S - i\frac{2f_T}{m_K}\sigma_{\alpha\beta}P_K^\alpha P_\pi^\beta]v(p_l)$ It consists of scalar, vector and tensor terms. $f_\pm$ are the functions of $t = (P_K - P_\pi)^2$. In the Standard Model (SM) the W-boson exchange leads to the pure vector term. The term in the vector part, proportional to f_- is reduced(using the Dirac equation) to a scalar form-factor, proportional to $(m_l/2m_K)f_-$ and is negligible in the case of K_{e3}. Different parametrizations have been used for $f_+(t)$. First is just a Taylor series: $f_+(t) = f_+(0)(1 + \lambda'_+ t/m_\pi^2 + \frac{1}{2}\lambda''_+ t^2/m_\pi^4)$. It is usually used to compare with ChPT predictions. Alternative parametrization is the pole one: $f_+(t) = f_+(0)\frac{m_V^2}{m_V^2 - t}$. The last is a relatively new Dispersive parametrization [5]: $f_+(t) = f_+(0)exp(\frac{t}{m_\pi^2}(\Lambda_+ + H(t)))$. Here H(t) is a known function.
The procedure for the experimental extraction of the parameters λ_+, f_S, f_T, which was developed in [6] is used. This procedure allows avoiding systematic errors due to the "migration" of the events over the Dalitz plot because of the finite experimental resolution. The radiative corrections were taken into account by reweighting every MC event, according to [7].

4.2. Results and comparison with theory
The results of the fit are summarized in Table 1. The first line is just a linear fit, it gives average slope of the $f_+(t)$ formfactor. It could be compared to quite old $ChPT$ $O(p^4)$ result [8]: $\lambda_+^{ChPT} = (31.0 \pm 0.6) \times 10^{-3}$. The second line is the "standard" fit with two parameters - linear and quadratic slopes. The quadratic term is quite significant, there is a strong correlation between parameters as it is seen in Fig. 3. The $ChPT$ $O(p^6)$ prediction for the quadratic slope is [9]: $\lambda''_+(ChPT) = (1.1 \pm 0.1) \times 10^{-3}$. The quality of the fit is illustrated by the z projection of the Dalitz plot, shown on Fig. 3. The third and fourth lines of the Table 1. correspond to the fits, when on top of the standard V-A term the scalar or tensor terms are allowed. In the fourth line, the correlation between F_S and F_T is used, inspired by a LeptoQuark model. It is seen, that f_S and f_T are not significant. The main contribution to systematic is coming from the variation of the cut on -z- coordinate of the vertex and the cut on the angle α. The systematic errors are shown in the Table 1. as the second error. The result of the Pole fit is: $M_V = 890 \pm 3.7$ MeV. It can be compared to the PDG value for the mass of K^* [10]: $M_{K*} = 891.66 \pm 0.26$ MeV. The Dispersion fit gives $\Lambda_+ = (24.72 \pm 0.23) \times 10^{-3}$. An interpretation of limits on F_S and F_T is possible in the framework of the scalar LeptoQuark(LQ) model. Then a diagram with LQ

Table 1. The results of the fits of the $f_+(t), f_S, f_T$ formfactors.

$\lambda'_+ \times 10^3$	$\lambda''_+ \times 10^3$	$f_S/f_+(0) \times 10^2$	$f_T/f_+(0) \times 10^2$
29.56± 0.28	0	0	0
26.1 ± 0.45 ± 0.38	1.94± 0.23 ± 0.12	0	0
26.1 ± 0.45 ± 0.38	1.93 ± 0.24± 0.12	-0.44 ± 0.7± 0.24	0.16 ± 2± 1.3
26.1 ± 0.45± 0.38	1.93 ± 0.24± 0.12	-0.41 ± 0.37± 0.24	0

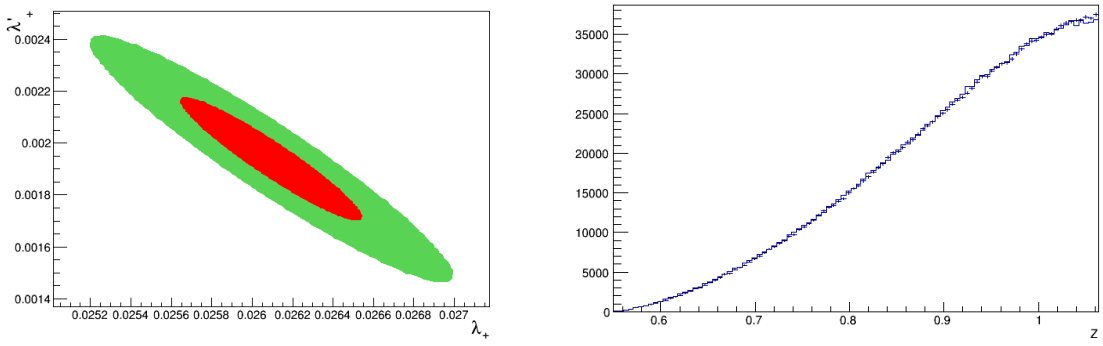

Figure 3. $\lambda' - \lambda''$ correlation plot (left); Projection of the Dalitz-plot on z (right) axis. Data is the points with errors; histogram is the fit, corresponding to the 2-nd line of the Table 1.

exchange should be added to the SM diagram with W. Applying Fiertz transformation to the LQ matrix element we get: $(\bar{s}\mu)(\bar{\nu}u) = -\frac{1}{2}(\bar{s}u)(\bar{\nu}\mu) - \frac{1}{8}(\bar{s}\sigma_{\alpha\beta}u)(\bar{\nu}\sigma^{\alpha\beta}\mu)$. The first term is the scalar, the second one - tensor. The relation between f_S, f_T and the Leptoquark scale Λ_{LQ} can be set out ([11]). As a result, a 95% lower limit for the LeptoQuark scale is $\Lambda_{LQ} > 3.5$ TeV.

5. Search for heavy neutrino in $K \to \mu\nu_H$ decay.

Two prescaled triggers are used for this study: $Tr_\mu = S_1 \cdot S_2 \cdot S_3 \cdot \overline{\check{C}}_1 \cdot \check{C}_2 \cdot \overline{S}_{bk} \cdot S_\mu/4$ and $Tr_{Kdec} = S_1 \cdot S_2 \cdot S_3 \cdot \overline{\check{C}}_1 \cdot \check{C}_2 \cdot \overline{S}_{bk}/10$, where S_μ is .OR. of 4 muon counters. Statistics of the November 2012 run is used for this analysis. One beam and one secondary track, identified as muon in GAMS, HCAL and muon counters are selected; decay vertex is required to be well inside the decay volume; total energy in the decay volume veto and in the large angle EGS e.m. calorimeter is required to be $E_{VETO} < 50$ MeV and $E_{EGS} < 100$ MeV. At this stage, $\sim 46M$ events are selected. Then several strong quality cuts are introduced for the beam and secondary track, which improve the missing mass resolution and suppress the background in the signal region. At this stage, we are left with $\sim 16M$ events. The distribution of the events over missing mass squared is shown in the left part of Fig. 4 together with the signal $K_{\mu 2}$ MC distribution and the MC backgrounds $K_{\mu 2\gamma}$; $K_{\mu 3}$; $K_{\pi 2}$. The results of the fit of the experimental distribution by the sum of the signal and the backgrounds is shown as well. The fit is good, as it is demonstrated by the residual distribution of the Fig. 4 (right). It is seen, that there is no significant extra signal from the heavy neutrino. To derive the upper limits, the residual spectrum is fitted by the gauss distributions with different masses and the MC-predicted width, which depends on the mass. From that, the one-sided 90% C.L. upper limits are constructed.

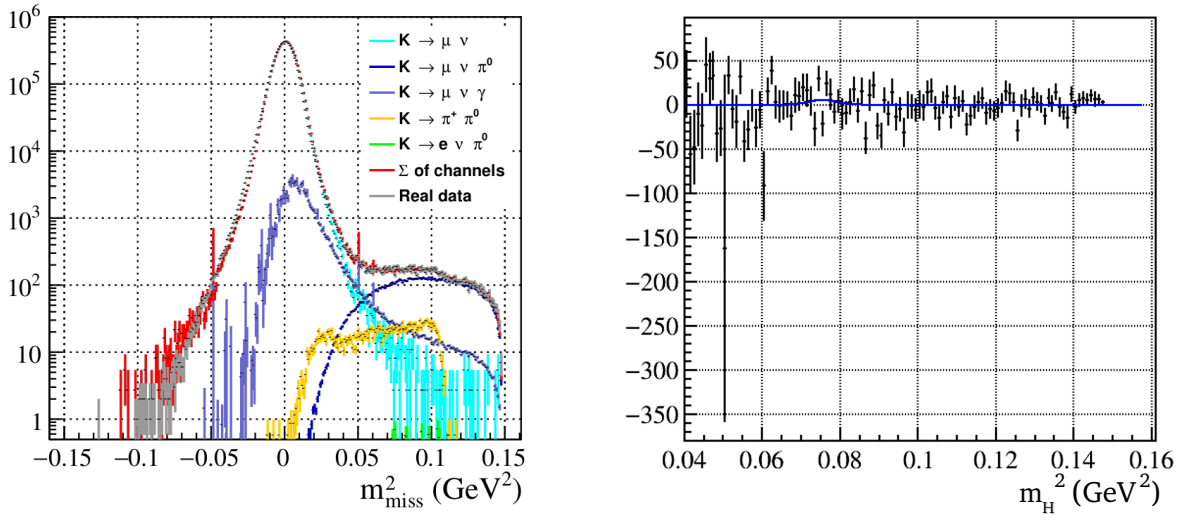

Figure 4. The missing mass squared for the selected events (left). The MC distributions for different components are also shown. Residuals distribution for the fit of the experimental data by the sum of $K_{\mu 2}$ and $K_{\mu 2\gamma}; K_{\mu 3}; K_{\pi 2}$ (right).

Using that, and normalizing to the $K \to \mu\nu$ it is straightforward to obtain the upper limit for the branching for $K^+ \to \mu^+\nu_H$, which is shown in the left part of Fig. 5 and, finally, the upper limits for the mixing parameter $|U_{\mu H}|^2$, shown in the right part of Fig. 5. The last figure also shows the previous limits obtained by KEK E-010 experiment [12] and BNL-949 experiment [13]. It is seen, that our limits extend the excluded region up to ~ 375 MeV. The cosmological limit (BBN) is also shown [14] .

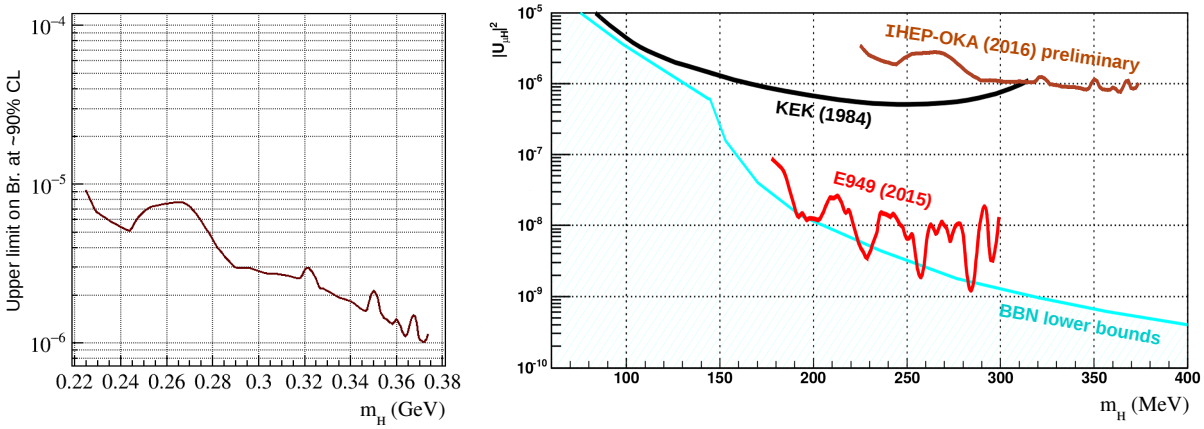

Figure 5. The 90% C.L. upper limits for the branching $K^+ \to \mu^+\nu_H$ (left); 90% C.L. upper limits for the mixing parameter $|U_{\mu H}|^2$ (right). Existing limits from KEK E-010 and E949 BNL experiments together with the cosmological limit (BBN) are shown.

6. Study of the $K^+ \to \pi^0\mu^+\nu\gamma$ decay.

This decay was first seen by ISTRA+ [15] and KEK K470 [16] in 2006. The decay is interesting, in particular, because one can build up a non-zero T-odd correlation from the momenta of the

particles $\xi = \vec{p}_\gamma \cdot (\vec{p}_\mu \times \vec{p}_\pi)/m_K^3$ and measure corresponding asymmetry $A_\xi = \frac{N(\xi>0)-N(\xi<0)}{N(\xi>0)+N(\xi<0)}$. There are calculations in χPT O(p4), in particular for the T-odd asymmetry [17]. For some extensions of SM $A_\xi \sim 3 \times 10^{-4}$ is expected. Statistics of 2012 and 2013 runs is used for the analysis. The selection requires one charged track identified as muon in GAMS, HCAL and μ-counters; then 3 extra showers are required, two of them from π^0 $0.11 < M_{\gamma\gamma} < 0.16$ GeV; missing momentum is required to point to active area of GAMS; total energy in veto is required to be $E_{VETO} < 50$ MeV and $E_{EGS} < 100$ MeV; to suppress $K^+ \to \pi^+\pi^0\pi^0 (K_{\pi 3})$ background two cuts are introduced $M^2_{miss} < 0.014$ or $M^2_{miss} > 0.0225$ GeV^2 ; finally the energy of the third photon in the kaon rest frame is required to be $E_\gamma > 30$MeV to suppress the $K_{\mu 3}$ background. The resulting distribution over $\mu\pi^0\gamma\nu$ mass, calculated assuming $m_\nu = 0$ is presented in Fig. 6. The number of signal events from the fit is ~ 580, which is about 4 times larger than in previous measurements. Using $K_{\mu 3}$ events for the normalisation we get $R = Br(K^+_{\mu 3\gamma}, 30 < E_\gamma < 60 MeV)/Br(K_{\mu 3}) = (4.85 \pm 0.2(stat) \pm 0.5(syst)) \times 10^{-4}$ which should be compared with 4.7×10^{-4} from the theory. An estimate of the T-odd asymmetry gives $A_\xi = (-0.19 \pm 0.05 \pm 0.09)$. A space asymmetry over $cos(\theta^*_{\mu\gamma})$, where $\theta^*_{\mu\gamma}$ is the angle between photon and muon momenta in the kaon rest frame is measured to be $A(cos\theta^*) = 0.6 \pm 0.05 \pm 0.1$.

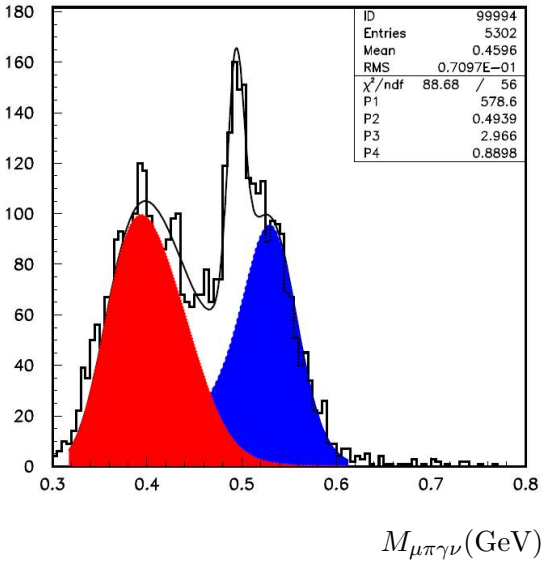

Figure 6. The invariant mass of the $\mu\pi^0\gamma\nu$ system calculated assuming $m_\nu = 0$.
A fit with 3 components: the residual background from $K_{\mu 3}$ (blue) ; $K_{\pi 3}$ (red) and the signal $K_{\mu 3\gamma}$ is shown.

References

[1] Garkusha V I et al. 2003 *Preprint* IHEP 2003-4.
[2] Citron A et al. 1979 *Nucl. Instr. and Meth.* **164** 31.
[3] Ageev A et al. 2008 *Proceedings of RUPAC* 282.
[4] Steiner H et al. 1971 *Phys. Lett.* B **36** 521.
[5] Bernard V et al. 2006 *Phys. Lett.* B **638** 480; Bernard V et al. 2009 *Phys.Rev.* D **80** 034034.
[6] Yushchenko O P et al. 2004 *Phys. Lett.* B **589** 111.
[7] Cirigliano V et al. 2002 *Eur. Phys. J.* C **23** 121.
[8] Gasser J and Leutwyler H 1985 *Nucl. Phys.* B **250** 517.
[9] Bijnens J,Talavera P 2003 *Nucl. Phys.* B **669** 341.
[10] Olive K A et al. 2014 *Chin. Phys.* C **38** 090001.
[11] Kiselev V V, Likhoded A K and Obraztsov V F 2002, *hep-ph*/0204066/.
[12] Asano Y et al. 1981 *Phys. Lett.* B **104**.
[13] Artamonov A V et al. 2015 *Phys. Rev.* D **91** 059903.
[14] Gorbunov D and Shaposhnikov M 2007 *JHEP* **0710** 015.
[15] Tchikilev O G et al. 2007 *Phys. Atom. Nucl.* **70** 29.
[16] Shimizu S et al. 2006 *Phys. Lett.* B **633** 190.
[17] Braguta V et al. 2003*Phys. Rev.* D **68**.